the plant journal

SEB Society for Experimental Biology

The Plant Journal (2017) **89,** 141–154 doi: 10.1111/tpj.13352

Isolation and characterization of mutants corresponding to the MENA, MENB, MENC and MENE enzymatic steps of 5′-monohydroxyphylloquinone biosynthesis in *Chlamydomonas reinhardtii*

Barbara Emonds-Alt[1], Nadine Coosemans[1], Thomas Gerards[2], Claire Remacle[1] and Pierre Cardol[1,*]

[1]*Department of Life Sciences, Genetics and Physiology of Microalgae, PhytoSYSTEMS, InBios, University of Liège, B–4000 Liège, Belgium, and*

[2]*Department of Life Sciences, Bioenergetics, PhytoSYSTEMS, InBios, University of Liège, B–4000 Liège, Belgium*

Received 15 June 2016; accepted 26 August 2016; published online 5 December 2016.
*For correspondence (e-mail pierre.cardol@ulg.ac.be).
Accession Numbers: Accession numbers are listed in Table 1.

SUMMARY

Phylloquinone (PhQ), or vitamin K_1, is an essential electron carrier (A_1) in photosystem I (PSI). In the green alga *Chlamydomonas reinhardtii*, which is a model organism for the study of photosynthesis, a detailed characterization of the pathway is missing with only one mutant deficient for MEND having been analyzed. We took advantage of the fact that a double reduction of plastoquinone occurs in anoxia in the A_1 site in the *mend* mutant, interrupting photosynthetic electron transfer, to isolate four new phylloquinone-deficient mutants impaired in *MENA*, *MENB*, *MENC* (*PHYLLO*) and *MENE*. Compared with the wild type and complemented strains for *MENB* and *MENE*, the four *men* mutants grow slowly in low light and are sensitive to high light. When grown in low light they show a reduced photosynthetic electron transfer due to a specific decrease of PSI. Upon exposure to high light for a few hours, PSI becomes almost completely inactive, which leads in turn to lack of phototrophic growth. Loss of PhQ also fully prevents reactivation of photosynthesis after dark anoxia acclimation. *In silico* analyses allowed us to propose a PhQ biosynthesis pathway in *Chlamydomonas* that involves 11 enzymatic steps from chorismate located in the chloroplast and in the peroxisome.

Keywords: *Chlamydomonas reinhardtii*, phylloquinone, insertional mutagenesis, anoxia, photosynthesis.

INTRODUCTION

In cyanobacteria, algae and land plants, photosynthetic electron transfer is driven by two large intrinsic protein complexes, photosystem I (PSI) and photosystem II (PSII), embedded in the thylakoid membrane. Each PS possesses several cofactors, including quinones (benzoquinone or naphthoquinone derivatives), that are required for electron transfer. Plastoquinone (PQ) is a benzoquinone derivative located in PSII (with two binding sites, Q_A and Q_B) and in the PQ pool. PQ is doubly reduced into plastoquinol (PQH_2) at the Q_B site and diffuses in the membrane to join the PQ pool so allowing the reduction of cytochrome b_6f complex (cyt b_6f) (Rochaix, 2002). In contrast, naphthoquinone derivatives participate in electron transfer within PSI. PSI is composed of two core subunits, PsaA and PsaB, containing 11 transmembrane domains and forming the heterodimeric reaction center that coordinates the cofactors required for electron transfer (Rochaix, 2002). The primary PSI electron donor is a dimer of chlorophyll *a* (P_{700}) located on the luminal side of the membrane. Electron transfer from P_{700} to ferredoxin occurs via chlorophyll A_0, naphthoquinone A_1 and three iron–sulfur centers [4Fe–4S], denoted F_X, F_A and F_B. Two naphthoquinones are present per P_{700} and allow electron transfer from A_0 to F_X by two branches (A and B) (Joliot and Joliot, 1999; Guergova-Kuras *et al.*, 2001). To date three types of 2-methyl-1,4-naphthoquinone derivatives, also known as vitamin K, have been identified in different oxygenic photosynthetic organisms. They share the same naphthalene nucleus but differ in the prenyl side-chain attached at position 3: menaquinone-4 (vitamin K_2) found in bacteria, diatoms and

primitive red algae (Yoshida *et al.*, 2003; Ikeda *et al.*, 2008) has a fully unsaturated C_{20} isoprenoid side-chain; phylloquinone (PhQ; vitamin K_1) found in most cyanobacteria, green algae and land plants, has a phytyl side-chain (partially saturated C_{20} prenyl); while 5′-monohydroxyphylloquinone (OH-PhQ) is found in *Euglena gracilis* and in some cyanobacteria like *Synechococcus elongatus* (Law *et al.*, 1973; Omata and Murata, 1984). Some species, such as the green microalga *Chlamydomonas reinhardtii*, possess two types of naphthoquinones: PhQ and OH-PhQ (Ozawa *et al.*, 2012). In *C. reinhardtii*, PhQ and OH-PhQ account for 10 and 90% of the total naphthoquinone content, respectively. Both are functional and contribute to photosynthetic electron transfer (Ozawa *et al.*, 2012).

Over the past decade the conversion of chorismate to menaquinone has been characterized in detail in bacteria (Meganathan, 2001; Jiang *et al.*, 2007, 2008; Chen *et al.*, 2013). Since the different types of naphthoquinones are structurally similar, most of the components of the PhQ biosynthesis pathway in the cyanobacterium *Synechocystis* sp. PCC 6803 have been identified by searching the cyanobacterial genome using bacterial genes as queries. In *Synechocystis*, nine enzymes, characterized by reverse genetics, catalyze the same steps as those required for synthesis of menaquinone: MenF (isochorismate synthase), MenD [2-succinyl-5-enolpyruvyl-6-hydroxy-3-cyclohexene-1-carboxylic acid (SEPHCHC) synthase], MenH [2-succinyl-6-hydroxy-2,4-cyclohexadiene-1-carboxylate (SHCHC) synthase], MenC (*o*-succinylbenzoic acid synthase), MenE (*o*-succinylbenzoyl-CoA ligase), MenB [1,4-dihydroxy-2-naphthoate (DHNA) synthase], Slr0204 [1,4-dihydroxy-2-naphthoate (DHNA)-CoA thioesterase], MenA (DHNA phytyltransferase) and MenG (methyltransferase) (Table 1) (Johnson *et al.*, 2000, 2001; Widhalm *et al.*, 2009).

In *Synechocystis*, inactivation of *menA*, *-B*, *-D* and *-E* genes leads to the complete absence of PhQ, which is replaced by PQ in the A_1 site of PSI (Johnson *et al.*, 2000, 2001, 2003; Semenov *et al.*, 2000). This substitution leads to delayed electron transfer from A_1^- to F_X because the redox potential of PQ in the A_1 site is more oxidizing than native PhQ, rendering electron transfer thermodynamically unfavorable. These mutants grow slowly under low-light conditions and are sensitive to high light. In contrast, inactivation of *menG*, the last enzyme of the PhQ biosynthetic pathway, results in the accumulation of demethylphylloquinone which replaces PhQ in PSI (Sakuragi *et al.*, 2002). The *menG* mutant is characterized by normal growth, although electron transfer from A_1^- to F_X is three times slower. All *Synechocystis men* mutants are characterized by a decreased PSI/PSII ratio but only under high light for *menG*.

Mutants deficient in the PhQ biosynthesis pathway have also been identified in photosynthetic eukaryotes. In *Arabidopsis thaliana*, inactivation of *ABC4* (the *menA* homolog) leads to a significant decrease in PSII, PSI, and content, (Shimada *et al.*, 2005). Mutants in the *PHYLLO* gene (which encodes a fusion of four eubacterial *men*-homologous regions corresponding to *menF*/*menD*/*menC*/*menH* genes) have drastically reduced PSI levels (5–15%) with nearly normal levels of PSII, and accumulate 55% of PQ (Gross *et al.*, 2006). Mutants with deletion of the *AAE14* gene (*menE* homolog), *ABC4* and *PHYLLO*, exhibit a

Table 1 Menaquinone biosynthesis enzymes in *Escherichia coli* and their homologs involved in the biosynthesis of phylloquinone (PhQ) in *Synechocystis*, *Arabidopsis* and *Chlamydomonas*

	E. coli	*Synechocystis* sp. PCC6803	*A. thaliana*	*C. reinhardtii*	E-value[a]
Isochorismate synthase	MenF	Slr0817	At1 g74710 (ICS1) At1 g18870 (ICS2)	Cre16.g659050 (PHYLLO)	6.4×10^{-74}
SEPHCHC synthase	MenD	Sll0603	At1 g68890 (PHYLLO)	Cre16.g659050 (PHYLLO)	6.4×10^{-74}
SHCHC synthase	MenH	Slr1916	At1 g68890 (PHYLLO)	Cre16.g659050 (PHYLLO)	6.4×10^{-74}
OSB synthase	MenC	Sll0409	At1 g68890 (PHYLLO)	Cre16.g659050 (PHYLLO)	6.4×10^{-74}
OSB–CoA ligase	MenE	Slr0492	At1 g30520 (AAE14)	Cre01.g030900 (MENE)	1.3×10^{-58}
DHNA synthase	MenB	Sll1127	At1 g60550 (NS)	Cre02.g114250 (MENB)	1.9×10^{-151}
DHNA-CoA thioesterase	YdiI	Slr0204	At1 g48320 (AtDHNAT1) At5 g48950 (AtDHNAT2)	Cre07.g323150[b] (TEH4) (putative)	–[b]
DHNA phytyltransferase	MenA	Slr1518	At1 g60600 (ABC4)	Cre04.g219787 (MENA)	2.6×10^{-14}
Demethylphylloquinone oxidoreductase	–[c]	Slr1743 (NdbB)	At5 g08740 (NDC1)	Cre16.g671000 (NDA5) (putative)	4.5×10^{-73}
Demethylphylloquinone methyltransferase	MenG	Sll1653	At1 g23360 (AtMenG)	Cre02.g084300 (MENG) (putative)	3.3×10^{-75}

[a]E-values from BLAST analysis with Arabidopsis protein sequences against the *Chlamydomonas* genome (version 5.5).
[b]No homolog has been found in the *C. reinhardtii* genomic database for the DHNA–CoA thioesterase described in *Synechocystis* and Arabidopsis. TEH4 is a putative candidate (see Discussion for further details).
[c]The penultimate reduction step of PhQ biosynthesis has not yet been demonstrated in menaquinone biosynthesis in bacteria.

seedling-lethal phenotype (Kim, 2008). In contrast, the Arabidopsis *menG*-homologous deficient mutant is viable because, as in *Synechocystis*, demethylphylloquinone acts as substitute for PhQ in PSI (Lohmann *et al.*, 2006). In 2015 it was established in *Synechocystis* and Arabidopsis that the biosynthesis of PhQ has an additional step: the reduction of the demethylphylloquinone ring by a type-II NADPH dehydrogenase, called NdbB in *Synechocystis* and NDC1 in Arabidopsis, prior to its *trans*-methylation by MenG (Fatihi *et al.*, 2015). *Synechocystis ndbB* and Arabidopsis *ndc1* mutants display increased photosensitivity to high light like the PhQ-deficient mutants previously characterized in these organisms.

In the green alga *C. reinhardtii*, which is a model organism for studying the photosynthetic machinery (Hippler *et al.*, 1998), characterization of the PhQ biosynthetic pathway is still incomplete. Up to now, only one mutant, deficient for MEND protein, has been characterized (Lefebvre-Legendre *et al.*, 2007). Inactivation of *MEND* in *C. reinhardtii*, as in *Synechocystis* sp. PCC 6803 (Johnson *et al.*, 2003), leads to the complete loss of PhQ and its replacement by PQ in PSI. However, accumulation of PSI is not affected in this mutant and the absence of PhQ rather causes a decrease in the size of the PQ pool and of synthesis of PSII subunits.

The phenotype of the only mutant isolated in *C. reinhardtii* is thus neither close to the one described in cyanobacteria or to that of land plants. This observation prompted us to isolate new mutants of the PhQ biosynthetic pathway in *C. reinhardtii.* In anoxia, a double reduction of PQ into PQH_2 in the A_1 site occurs in the *mend* mutant, interrupting photosynthetic electron transfer (Lefebvre-Legendre *et al.*, 2007; McConnell *et al.*, 2011). In this work, we took advantage of this photosynthetic deficiency in anoxia to isolate four new *Chlamydomonas* mutants affected in either the MENA, MENB, MENC or MENE enzymatic step of the PhQ biosynthesis pathway.

RESULTS

A peculiar chlorophyll induction curve is specific for identification of PhQ-deficient mutants

Nine sequences corresponding to nine of the ten enzymatic steps required for the PhQ biosynthesis pathway in cyanobacteria and land plants can be found in the *C. reinhardtii* genomic database (v.5.5 on PHYTOZOME) (Table 1). Genomic sequences coding for MENF, MEND, MENC and MENH enzymatic domains are located in a single open reading frame (ORF), and are named *PHYLLO* by similarity to gene organization in *A. thaliana* (Gross *et al.*, 2006), and likely coding for a tetramodular enzyme. We did not find any homolog to the DHNA-CoA thioesterase performing the seventh step of the pathway in cyanobacteria and land plants but a putative candidate (TEH4) is suggested (see Discussion).

To isolate new *C. reinhardtii* strains deficient in PhQ biosynthesis we screened 13 250 hygromycin-resistant (Hyg^R) transformants and 3500 paromomycin-resistant (Par^R) transformants by an *in vivo* chlorophyll fluorescence imaging screening protocol. The screening procedure is based on the observation that a double reduction of PQ in PQH_2 in the A_1 site occurs in a *mend* mutant in anoxia, interrupting photosynthetic electron transfer (McConnell *et al.*, 2011). We thus recorded the chlorophyll fluorescence induction curves of transformants after prolonged dark incubation under anoxia. As previously described (Godaux *et al.*, 2013), for dark anoxic-acclimated wild-type cells, F_O is close to F_M, which indicated that the PSII acceptor pool (Q_a, PQ) is largely reduced. Upon illumination, the fluorescence yield reaches a maximum transient value in a few milliseconds and then decreases to a steady-state value after about 1 sec. The value of the PSII efficiency (ΦPSII), determined after 3 sec of illumination by addition of a saturating pulse, reached 0.5 (Figure 1a). Conversely, the electron transfer was blocked from the very beginning of illumination in the *mend* mutant, and ΦPSII after 3 sec of illumination is null (Figure 1a). We isolated here five Hyg^R (AL2, AO1, AO2, AS1, AS2) and two $Paro^R$ mutants (24.1, 25.1) with a similar chlorophyll fluorescence induction curve to *mend* (Figure 1b). In contrast, the behavior of these mutants is almost identical to the wild type in control conditions (oxic) (Figure 1c). This suggested that these mutants were specifically impaired in PhQ biosynthesis.

To determine whether the fluorescence phenotype of these mutants is linked to the antibiotic-resistance cassette, a genetic cross between each mutant of mating-type plus (mt^+) was performed with the wild-type strain of the opposite mating type (mt^-) and phenotype of the meiotic progeny was analyzed (Table S1). For four mutants (AO1, AS1, AS2 and 25.1) all meiotic products that were resistant to antibiotic also showed the mutant fluorescence phenotype, while all meiotic products that were sensitive to the presence of antibiotics behaved like the wild type. In addition, around half of the meiotic progeny were resistant to antibiotics in each of the four crosses. This suggested that a unique functional cassette was linked to the phenotype of each individual mutant. In contrast, the presence of four classes of meiotic products in the progeny of AL2, AO2 and 24.1 indicated that the fluorescence phenotype was not directly linked to the insertion of the cassettes. As a consequence, these mutants (AL2, AO2 and 24.1) were discarded. To confirm that only one cassette was inserted in the genome of AO1, AS1, AS2 and 25.1 mutants, DNA gel-blot analysis was carried out on the four tagged mutant strains with specific probes against *APHVII* (for AO1, AS1 and AS2 mutants) and *APHVIII* (for the 25.1 mutant)

cassettes. As only one fragment was revealed after hybridization, we concluded that each mutant contained a single copy of the resistance cassette in its nuclear genome (Figure 2a). To determine the genomic DNA sequences flanking the insertion cassette for each individual mutant, we performed thermal asymmetric interlaced (TAIL) PCR and the resulting PCR products were sequenced (Figure S1 in the Supporting Information). A detailed description of this analysis is given in Appendix S1 and summarized in Figure 2(b). In brief, the four mutants are all affected in one of the genes of the putative PhQ biosynthetic pathway in *Chlamydomonas*: *MENA* (AS2, *mena* mutant), *MENB* (AS1, *menb* mutant), *PHYLLO* (AO1, *menc* mutant) and *MENE* (25.1, *mene* mutant).

We then aimed to obtain complemented strains as an additional proof of phenotype. To this end, we amplified *MENB* (4865 bp) and *MENE* (4177 bp) genes and their flanking regions (Figure S2). However, we could not amplify *MENA* (3136 bp). We did not try to amplify the corresponding gene for *PHYLLO* (15.7 kb) because it was too long to be amplified by PCR. *menb* cells and *mene* cells were then co-transformed using the appropriate selection marker (*APHVIII* or *APHVII*, respectively) and the PCR product containing the *MENB* or *MENE* gene, respectively. Transformants were selected on medium containing both hygromycin and paromomycin and co-transformants which had incorporated and expressed the second marker (either *MENB* or *MENE*) were selected on the basis of their restored wild-type fluorescence pattern after acclimation to dark anoxic conditions (Figure S3). One complemented co-transformant was selected for each strain, and called *menbR* or *meneR,* respectively.

Absence of PhQ in the *men* mutant strains

To determine the impact of *mena*, *menb*, *menc* and *mene* mutations on PhQ abundance, pigments were extracted

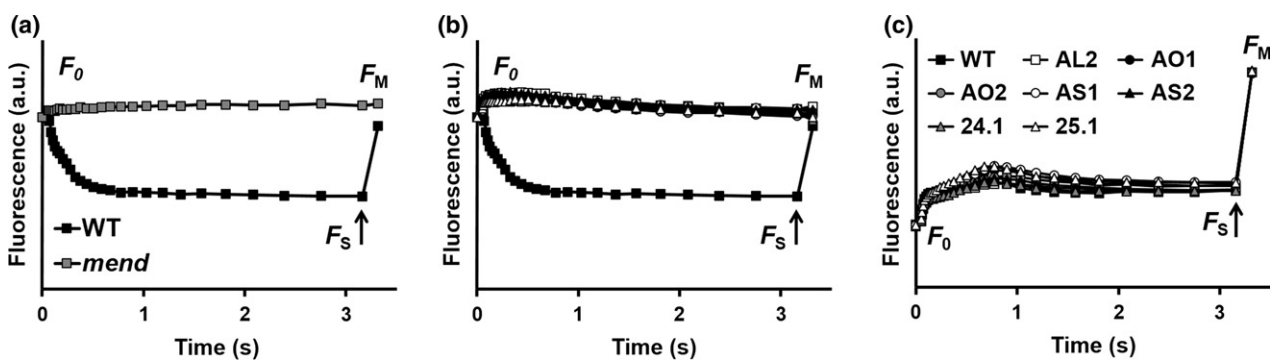

Figure 1. Chlorophyll fluorescence induction curves of wild-type and mutant strains.
Chlorophyll fluorescence induction curves upon illumination at about 110 μmol photons (λ = 520 nm) m^{-2} sec^{-1} of *Chlamydomonas reinhardtii* wild type, *mend* mutant and mutant strains identified in this work after acclimation to dark anoxic (>12 h) (a, b) and oxic conditions (c). Arrows indicate when the saturating light pulse was given.

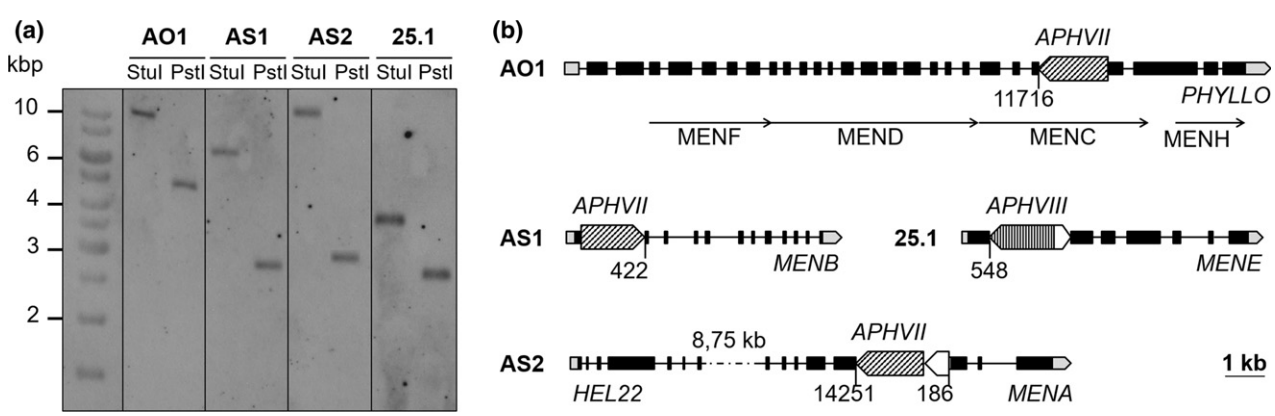

Figure 2. Molecular characterization of the mutants.
(a) DNA-blot analysis of wild-type and mutant strains. For AO1, AS1 and AS2, the DNA-blot was hybridized with a digoxigenin (DIG)-labeled *APHVII* probe, while for 25.1 the DNA-blot was hybridized with a *DIG*-labelled *APHVIII* probe.
(b) Organization and structure of the *MENA*, *MENB*, *MENE* and *PHYLLO* genes as shown in *Chlamydomonas reinhardtii* genome version 5.5 available at http://phytozome.org (black boxes, exons; black lines, introns; grey boxes, 5′ and 3′ UTRs; *men*-homologous regions, black pointer) and localization of the antibiotic resistance cassette (diagonally hatched arrows, *APHVII*; vertically hatched arrows, *APHVII*; white arrows, pieces of non-functional cassette).

from lyophilized cells and analyzed by ultra-performance liquid-chromatography mass spectrometry (UPLC-MS). The elution profile of the *men* mutant cell extracts was compared with those of wild-type and complemented cell extracts. Because about 90% of the total amount of naphthoquinones in *C. reinhardtii* is present as OH-PhQ (Ozawa *et al.*, 2012), we decided to focus on the detection of this form. OH-PhQ, whose determined *m/z* values for the non-adduct form and Na^+ adduct form are 467.35 and 489.33, respectively, was detected as a single peak at 8.06 min of the chromatogram of wild-type and complemented cell extracts. This peak was missing in the *men* mutant cell extracts (Figure 3), indicating loss of OH-PhQ.

Light response of PhQ-deficient mutants

Since the previously isolated *Chlamydomonas mend* mutant is light sensitive (Lefebvre-Legendre *et al.*, 2007), we analyzed the growth of *mena*, *menb*, *menc*, *mend* and *mene* mutant strains in the presence [2-amino-2-(hydroxymethyl)-1,3-propanediol (TRIS)-acetate-phosphate (TAP) medium] or the absence (TMP medium) of acetate. We concentrated on comparing growth at low and high light intensities for mutant and control strains. After 3 days of illumination, all mutants grew more slowly than the wild type and complemented strains, whatever the medium and the light conditions used (Figure 4). At day 7, this delayed growth was no longer observed on TAP medium in the dark and under low light (25 μmol photons m^{-2} sec^{-1}) but was still visible in the other conditions, e.g. under higher light (125 and 300 μmol photons m^{-2} sec^{-1}) in the presence (TAP) or in the absence (TMP) of acetate in the medium. In addition, it has been shown that growth of *mend* could be partially restored by the addition of exogenous PhQ at high light intensities (Lefebvre-Legendre *et al.*, 2007). This was also the case for *menb*, *menc* and *mene* mutants, suggesting that the three mutants are auxotrophic for PhQ. In contrast, the addition of exogenous PhQ had no effect on the growth of the *mena* mutant (Figure 4).

Reorganization of the photosynthetic apparatus in the absence of PhQ

In order to investigate the impact of a lack of PhQ on photosynthesis, we first determined the content of active PSI and PSII in mutant and control strains by a spectroscopic approach based on the magnitude of the electrochromic shift (ECS) induced by charge separation (Bailleul *et al.*, 2010). We observed a decrease of 30–40% in the active PSI centers in all mutant strains (Figure 5a). This decrease in active PSI content was further confirmed by assessing the relative concentration of P_{700} by redox difference spectroscopy (Figure S4) and by immunoblotting on a Western blot against PsaA protein (Figure 5c). Similarly, in line with previous immunoblotting experiments against PSII core proteins D1 and D2 (Lefebvre-Legendre *et al.*, 2007), the amount of active PSII (Figure 5a) and core antenna subunit Cp43 (Figure 5c) was very low in the *mend* mutant. Conversely, no decline in PSII centers was observed in the four *men* mutants identified in this work (Figure 5a,c).

To gain information on the distribution of excitation energy between PSI and PSII, we also recorded the 77 K fluorescence emission spectra of whole *C. reinhardtii* cells. Excitation in the chlorophyll Soret band produces PSII and PSI fluorescence bands at 685 and 715 nm, respectively, each band resulting from fluorescence emission of different forms of PS–light harvesting complex (LHC) supercomplexes (e.g. ranging from 708 to 715 nm in the case of PSI; Drop *et al.*, 2011). In *men* mutant cells frozen to 77 K under the low white light used for growth, the relative amplitude of the 715-nm peak was larger than in the wild type and complemented strains (Figure 5g). This result suggests a relative increase in PSI antenna size in *men* mutant cells due to: (i) a larger LHCI or (ii) an association of LHCII with PSI (i.e. a transition to state II due to a more reduced state

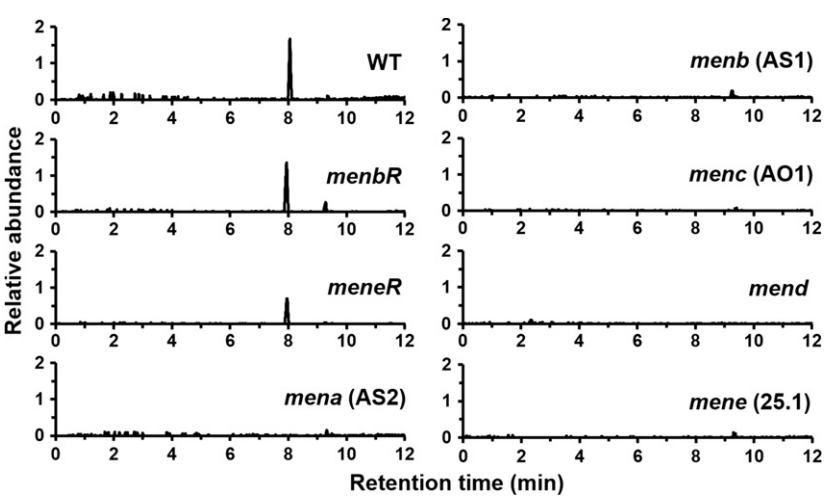

Figure 3. Analysis of phylloquinone content by ultra-performance liquid-chromatography mass spectrometry.
Detection of 5′-monohydroxyphylloquinone (selected monitoring mode, *m/z* = 488.5–489.5; retention time about 8 min) from wild type, complemented strains (*menbR*, *meneR*) and *men* mutants. Values are normalized to the relative abundance of lutein (*m/z* = 568.43).

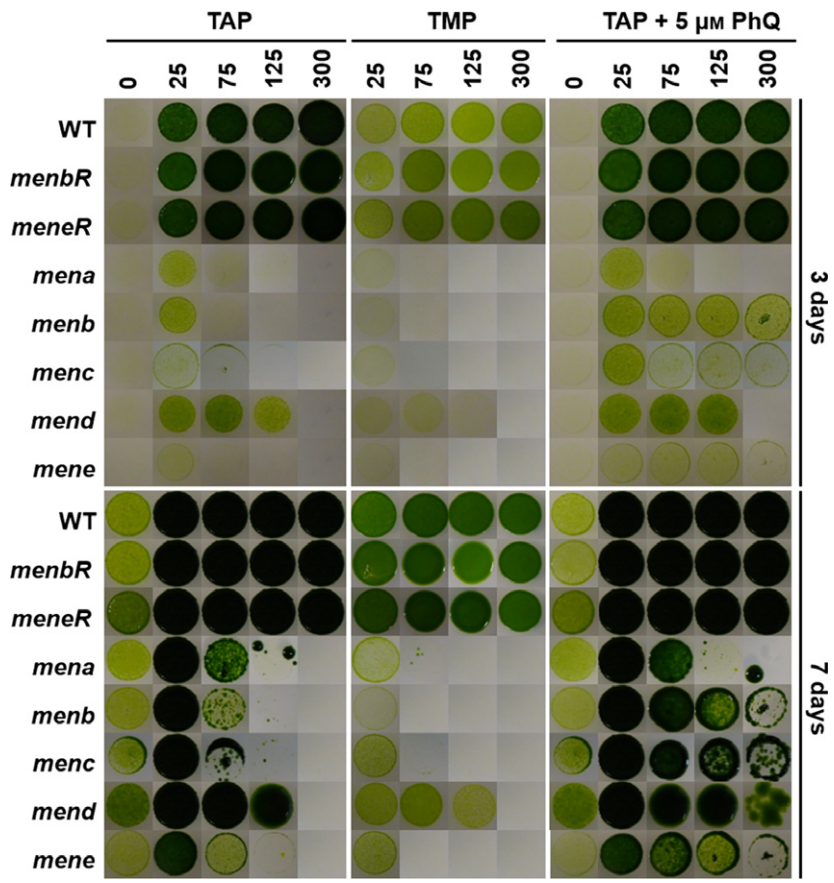

Figure 4. Growth of control and mutant strains under different culture conditions.
Growth patterns of the wild type (WT), complemented strains and *men* mutants. Twenty microliters of cell culture at 10^6 cells ml^{-1} was plated on acetate-containing medium (TAP), acetate-free medium (TMP) and TAP medium supplemented with 5 μM of phylloquinone (PhQ). Agar plates were incubated for 3 and 7 days under 0, 25, 75, 125 and 300 μmol photons m^{-2} sec^{-1}. The images for each experimental condition come from a single Petri dish with all strains, except *menc* which was compared with the wild type only.

of the PQ pool; Wollman, 2001). To test these hypotheses, we treated the cells with 3-(3,4-dichlorophenyl)-1,1-dimethylurea (DCMU) to inhibit PSII and to re-oxidize the PQ pool in the light, thus allowing re-association of LHCII and PSII (i.e. transition to state I) (Cardol *et al.*, 2003). In the wild type and complemented strains, this treatment leads to a full transition to state I, detected as a decrease in the relative amplitude of the 715-nm band. In contrast, DCMU-treated *men* cells still show a higher emission at 715 nm relative to 685 nm. To confirm this result, we measured PSI antenna size at state I using ECS (Bailleul *et al.*, 2010; Takahashi *et al.*, 2013). The initial slope of the ECS changes measured in continuous light and in the presence of DCMU (to inhibit PSII) can be used to probe the absorption cross-section of PSI because it is proportional to the light intensity (Figure S5a). An increase in PSI antenna size was observed in all *men* mutants compared with control strains (a 20–50% increase) (Figure 5h). In parallel, PSII antenna size was estimated from mid-rise values of the chlorophyll fluorescence transients measured in continuous light and in the presence of DCMU at state I (Figure S5b). PSII antenna size remained unchanged, with the exception of *mend* (70% increase) (Figure 5h).

We finally explored the impact of the imbalance in the PSI/PSII stoichiometry and antenna size of *men* mutants on the relative electron transfer rate at the PSII level ($rETR_{II}$). When cultivated in low light, *men* mutants exhibited a significant decrease of $rETR_{II}$ compared with the wild type and complemented strains (Figure 5e). A decrease of about 30% is observed for *mena* and *menb* mutants and of about 60% for *menc*, *mend* and *mene* mutants.

All spectroscopic experiments so far were carried out on algae grown under low light. In these conditions, *men* mutants are still able to grow (Figure 4) even if a decrease in the number of active PSI centers limits the photosynthetic electron flow. In contrast mutants are unable to grow under high light. We thus assumed the existence of additional deleterious effects on the photosynthetic chain in algal cells under high light. To test this hypothesis, wild-type and mutant cells were grown in low light (25 μmol photons m^{-2} sec^{-1}) and then transferred for 4 h to a high light intensity (400 μmol photons m^{-2} sec^{-1}). After 4 h in high light, the content of active PSI centers remained relatively constant in the wild type and complemented strains, but it progressively decreased over time in *mena*, *menb*, *menc* and *mene* to <10% of that of controls and in *mend* by half (Figures 5b and S6). Conversely, the number of active PSII centers already began to fall at a steady level after 1 h in high light in control strains (40–60% decrease) and *men* mutants (70–80% decrease) (Figures 5b and S6),

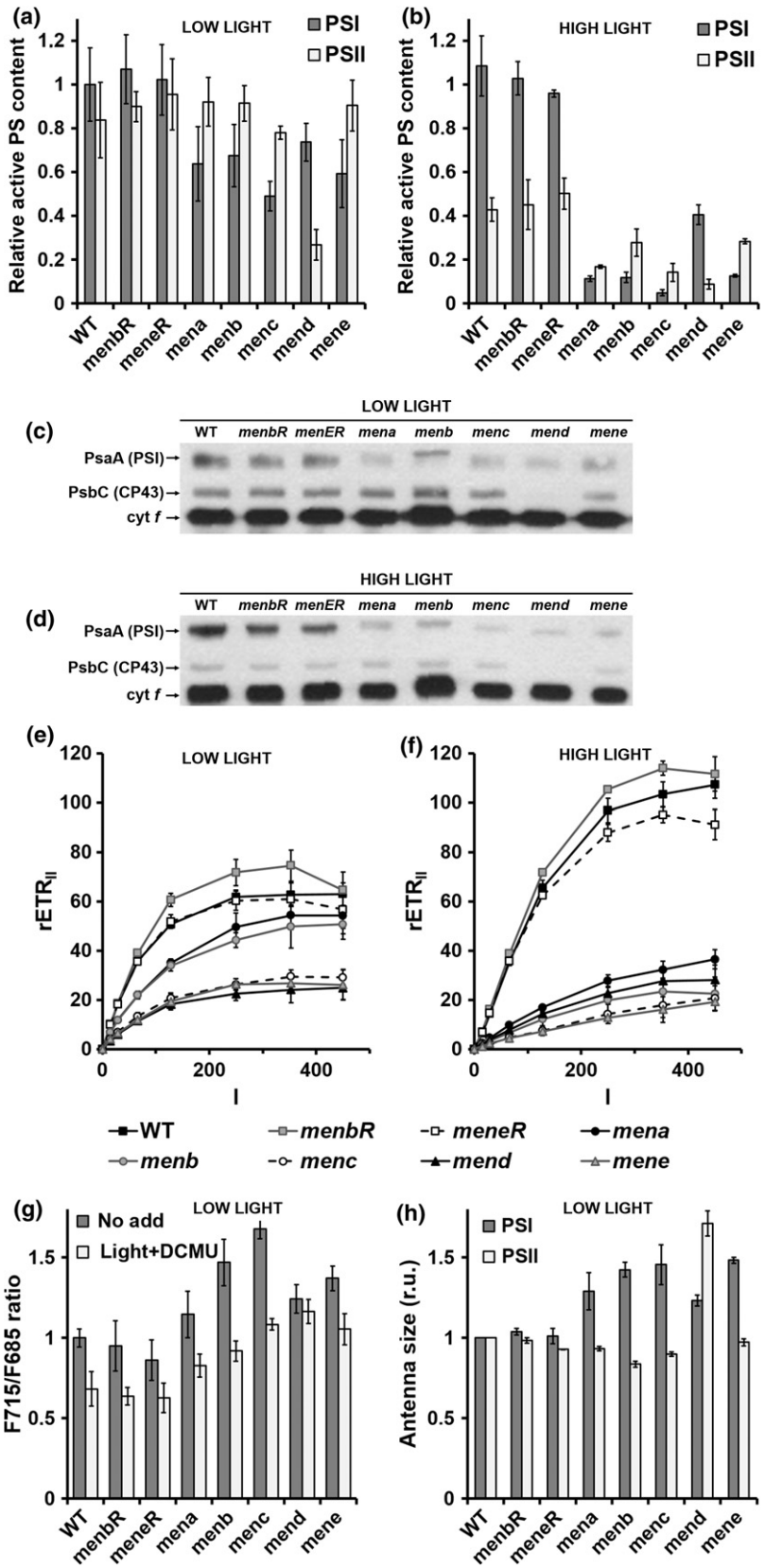

Figure 5. Photosystem content, antenna size and electron transfer rate in control and mutant strains.
(a), (b) Active photosystem (PS) I and PSII content was estimated from electrochromic shift signals (ECS) at 520–546 nm on cells grown in low light (a) and then transferred for 4 h to a high light intensity (HL; 400 μmol photons m^{-2} sec^{-1}) (b). The active PSI center content of wild-type (WT) cells was normalized to 1. Values are the average of three independent experiments. (c), (d) Immunoblots against *Chlamydomonas reinhardtii* PsaA, Cp43 and cytochrome *f* proteins of total cell extracts (5 μg protein per lane) prepared from wild-type, *menbR*, *meneR*, *mena*, *menb*, *menc*, *mend* and *mene* cells grown in low light (c) and then transferred for 4 h to high light (400 μmol photons m^{-2} sec^{-1}) (d). The antibodies used are indicated. (e), (f) The PSII relative electron transfer rate ($rETR_{II}$, μmol electrons sec^{-1} m^{-2}) as a function of the light intensity (*I*, μmol photons m^{-2} sec^{-1}) of cells grown in low light (e) and then transferred for 4 h to high light (400 μmol photons m^{-2} sec^{-1}) (f). In (e) and (f) values are the average of 10 independent experiments. (g) F715: F685 ratio from fluorescence emission spectra at 77 K. Different pre-treatments were applied to cell suspensions before freezing: control under white light of 25 μmol photons m^{-2} sec^{-1} ('no add', dark grey symbols) or illumination by white light of 25 μmol photons m^{-2} sec^{-1} in the presence of 20 μM 3-(3,4-dichlorophenyl)-1,1-dimethylurea (DCMU) ('light + DCMU', light grey symbols). (h) PSI antenna size estimated from ECS absorbance transients (520–546 nm) in DCMU (20 μM) + hydroxylamine (1 mM)-poisoned cells (Figure S5a) and PSII antenna size estimated from chlorophyll fluorescence transients in DCMU (20 μM)-poisoned cells (Figure S5b). In (g), (h) Wild-type values were normalized to 1 and all values are the average of three independent experiments.

indicating a more pronounced PSII photoinhibition in all *men* strains. Consistently, $rETR_{II}$ was drastically reduced in all *men* strains after 4 h under high light (to about 20% of the wild-type value) (Figure 5f).

To determine whether the decrease in the number of active PS is associated with a decrease in the total amount of PS per cell or to a loss of activity of PS centers present after exposure to high light (for 4 h), the amount of core subunit PsaA (PSI) and core antenna subunit Cp43 (PSII) were compared with the amount of cytochrome *f* (cytochrome b_6f complex) by immunodetection on Western blot on total cell extracts (Figure 5d). The PsaA content was lower in all *men* mutants, but this decrease was not especially pronounced in comparison with the decrease in the amount of PsaA observed for low-light-adapted *men* mutant cells. We conclude that the decrease of $rETR_{II}$ in the *men* mutant exposed to high light is thus due to a specific PSI photoinhibition.

It is notable that the *mend* mutant behaves slightly differently. Its PSII content is much lower in low light (Figure 5a,c), which is in agreement with its original description (Lefebvre-Legendre *et al.*, 2007). Upon exposure to high light, this reduced PSII content might limit electron flow to PSI, translating into a lower PSI photoinhibition compared with other *men* mutants (Figure 5b). In principle, both *menc* and *mend* mutants should be affected in the whole *PHYLLO* locus and thus should behave in exactly the same way. As a matter of proof, a RT-PCR experiment indicated that the mRNA segment corresponding to the MENC–MENH domain is absent in the *mend* mutant, as in the *menc* mutant (Figure S7). We tried to determine if a secondary mutation could be responsible for the partly rescued phenotype of *mend*, but unfortunately it was impossible to cross *mend* with our wild-type reference strains. We postulate that the *mend* mutant (Lefebvre-Legendre *et al.*, 2007) has been subject to adaptations that led to the observed decrease in PSII content and consequently to a lower PSI photoinhibition (Figures 5a,b and S6), and better growth (Figure 4).

DISCUSSION

The PhQ biosynthetic pathway might comprise 11 enzymatic steps located in the chloroplast and the peroxisome

Genomic data for *C. reinhardtii* (Table 1) indicate that the biosynthetic pathway of PhQ from chorismate comprises homologs for nine of the ten consecutive enzymatic steps involved in the biosynthesis of PhQ in *Synechocystis* sp. PCC 6803 and in *A. thaliana* (Fatihi *et al.*, 2015). We did not find any obvious homolog of the cyanobacterial and plant DHNA–CoA thioesterase in *Chlamydomonas* or in other green algae (e.g. *Chlorella vulgaris* C-169, *Chlorella* sp. NC64A, *Volvox carteri*). It is notable that the plant and cyanobacterial DHNA–CoA thioesterases are not encoded by homologous genes: the plant version originates from horizontal gene transfer with a bacterial species (Widhalm *et al.*, 2012). Altogether, this suggests that another thioesterase might operate in the PhQ biosynthesis pathway of green algae. Among the large family of thioesterases in *C. reinhardtii*, TEH4 (Cre07.g323150) is a possible candidate because it possesses the hot-dog domain typical of DHNA–CoA thioesterase (Furt *et al.*, 2013), a putative binding site for coenzyme A, and a peroxisomal targeting sequence (PTS) (see below for further discussion). In flowering plants, genetic approaches identified the *PHYLLO* locus, which codes for a multi-enzyme composed of four fused eubacterial *men*-homologous modules corresponding to MenF/MenD/MenC/MenH proteins, respectively (Gross *et al.*, 2006). Homology searches revealed the existence of cluster *PHYLLO* orthologs in green algae, mosses, diatoms and red algae (Gross *et al.*, 2006). The C-terminal region bearing the chorismate-binding site is absent from the PHYLLO MENF module in Arabidopsis, and isochorismate synthase (ICS) activity is performed by the products of the *ICS1* and *ICS2* genes (Gross *et al.*, 2006; Garcion *et al.*, 2008). PHYLLO then catalyzes consecutive reactions (MEND, -C and -H) that lead to the synthesis of *o*-succynilbenzoate (Gross *et al.*, 2006). In contrast to Arabidopsis PHYLLO protein, the *C. reinhardtii* nuclear genome likely encodes a PHYLLO tetramodular enzyme that would exhibit a full MENF chorismate-binding domain that might be functional (Figures 2b and S8). Accordingly, we thus assume that our *Chlamydomonas* mutants are impaired in the fourth (MENC), the fifth (MENE), the sixth (MENB) and the eighth (MENA) enzymatic steps of PhQ biosynthesis (Figure 6). The previously characterized *mend* mutant (Lefebvre-Legendre *et al.*, 2007) would be impaired in the second step. Even if the existence of a tetramodular PHYLLO enzyme remains to be demonstrated beyond genomic evidence, it is reasonable to consider at this stage that *menc* and *mend* mutants are impaired in the function of the whole PHYLLO multi-enzyme (i.e. including MENF and MENH activities).

Ultimately, four steps in *Chlamydomonas* remain to be characterized by genetic approaches: step 7 is the putative DHNA–CoA thioesterase TEH4; step 9 would be performed by the type II NADPH dehydrogenase NDA5 which is the homolog of Arabidopsis NDC1 and *Synechocystis* NdbB (Desplats *et al.*, 2009); step 10 is probably performed by the MENG homolog, and an ultimate additional step (step 11) of hydroxylation of PhQ to OH-PhQ, specific to some microalgae like *C. reinhardtii* and *Euglena gracilis* (Ziegler *et al.*, 1989; Ozawa *et al.*, 2012), also remains to be elucidated. In this regard, two cytochrome P450-dependent PhQ hydroxylases have been recently identified (CYP4F2 and CYP4F11) in humans (Edson *et al.*, 2013). A putative

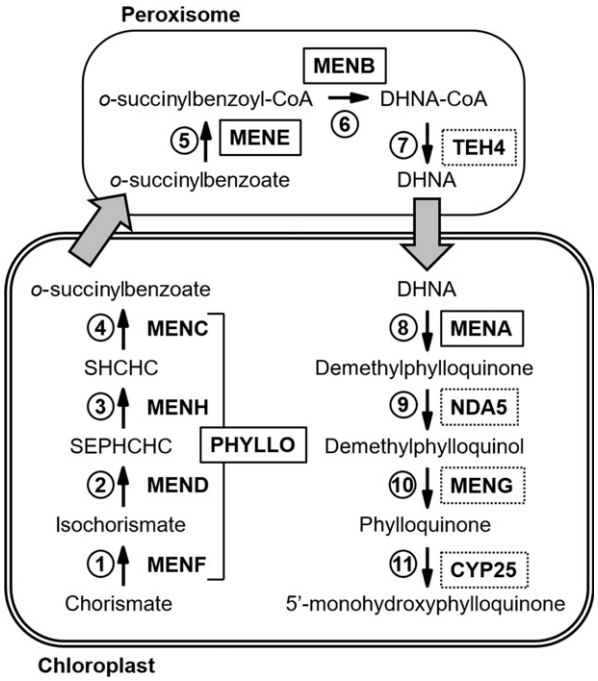

Figure 6. Phylloquinone biosynthetic pathway in *Chlamydomonas reinhardtii*.

The gene products encoding each step in *Chlamydomonas* are indicated. The PHYLLO protein contains catalytic domains corresponding to MenF, MenD, MenH and MenC of the menaquinone pathway. MENE, MENB and TEH4 possess peroxisome-targeting sequences suggesting a compartmentalized phylloquinone biosynthesis pathway similar to that of land plants (see text for details). Solid black boxes indicate that mutants have been characterized, dotted black boxes specify putative *men* proteins and grey arrows designate uncharacterized membrane trafficking steps (see text for details). MENF, isochorismate synthase; MEND, SEPHCHC synthase; MENH, SHCHC synthase; MENC, OSB synthase; MENE, OSB–CoA ligase; MENB, DHNA synthase; TEH4, putative DHNA–CoA thioesterase (DHNAT); MENA, DHNA phytyltransferase; NDA5, putative demethylphylloquinone oxidoreductase; MENG, putative demethylphylloquinone methyltransferase; CYP25, putative phylloquinone hydroxylase; SEPHCHC, 2-succinyl-5-enolpyruvyl-6-hydroxy-3-cyclohexene-1-carboxylic acid; SHCHC, 2-succinyl-6-hydroxy-2,4-cyclohexadiene-1-carboxylic acid.; OSB, *o*-succinylbenzoic acid; DHNA, 1,4-dihydroxy-2-naphthoate.

homolog (CYP25, Cre08.g373100) is present in *Chlamydomonas* (Figure S9) and could fulfil the role.

The location of the PhQ biosynthesis pathway in *Chlamydomonas* is also unknown. Mainly originating from the cyanobacterial ancestor, most of the proteins involved in biosynthesis of PhQ in Arabidopsis are located in the chloroplast (Shimada *et al.*, 2005; Gross *et al.*, 2006; Lohmann *et al.*, 2006; Garcion *et al.*, 2008; Kim, 2008). MenE/AAE14, however, has dual localization in the chloroplast and peroxisome (Kim, 2008; Babujee *et al.*, 2010), while MenB/NS and DHNA-CoA thioesterases are targeted to the peroxisome (Reumann *et al.*, 2007; Babujee *et al.*, 2010; Widhalm *et al.*, 2012). Here we took advantage of the recent identification of PTS motifs in *C. reinhardtii*, which are similar to Arabidopsis PTS (Lauersen *et al.*, 2016), to identify three PTS sequences among *Chlamydomonas* peptide sequences discussed in this work: PTS1 (SRL) in MENE and TEH4 C-terminal parts (position 732–734 and 201–203, respectively), and a PTS2 in MENB N-terminal part (RLqvlsnHL at position 7–15). This suggests that in *Chlamydomonas*, as in Arabidopsis, this part of the biosynthetic pathway also occurs in the peroxisome but this hypothesis remains to be confirmed by subcellular localization experiments. Altogether, our results suggest that localization of the steps involved in the PhQ biosynthesis pathway in *Chlamydomonas* (Figure 6) might be very similar to that previously described in land plants (Fatihi *et al.*, 2015), and that there is no alternative route for PhQ synthesis in *Chlamydomonas*. We thus propose that chorismate is converted into *o*-succinylbenzoate by the first four enzymatic steps (PHYLLO) in the chloroplast. Then, *o*-succinylbenzoate would be exported to the peroxisome where the succinyl chain would be activated by ligation with CoA and cyclized to yield 1,4-dihydroxy-2-naphthoyl (DHNA)–CoA. After hydrolysis of DHNA–CoA by an unknown thioesterase, possibly located in the peroxisome, the naphthoquinone ring would be conjugated to a phytyl chain. Finally, the demethylphylloquinone precursor would be reduced in demethylphylloquinol form, methylated into PhQ and hydroxylated into OH-PhQ in the chloroplast (Figure 6).

Lack of PhQ primarily affects PSI activity

Phylloquinone is an essential electron carrier in PSI. As previously demonstrated in *Chlamydomonas* and *Synechocystis*, PQ might replace the missing PhQ in the A_1 site of PSI, rendering the electron transfer from A_1^- to F_X thermodynamically unfavorable (Semenov *et al.*, 2000; Lefebvre-Legendre *et al.*, 2007; McConnell *et al.*, 2011). In this work, we have identified and characterized four new *C. reinhardtii* nuclear insertion mutants deficient for OH-PhQ, the predominant form of naphthoquinone in this species (Ozawa *et al.*, 2012). All *Chlamydomonas men* mutants (including the previously characterized *mend*; Lefebvre-Legendre *et al.*, 2007) can grow photoautotrophically under moderate light (25 μmol photons m^{-2} sec^{-1}) but are sensitive to high light. Arabidopsis *abc4* (MENA), *phyllo* (PHYLLO MENDCH), *aae14* (MENE) and double knockout *ics1*/*ics2* (MENF) mutants are also characterized by loss of phototrophy and a seedling lethal phenotype even in low light, but it is not known if missing PhQ is replaced by PQ in this species (Shimada *et al.*, 2005; Gross *et al.*, 2006; Garcion *et al.*, 2008; Kim, 2008). The Arabidopsis *meng* and *ndc1* mutants are the sole viable PhQ-deficient mutants in plants (Lohmann *et al.*, 2006; Fatihi *et al.*, 2015). *Synechocystis* and Arabidopsis *meng* and *ndc1* mutants accumulate demethylphylloquinone which replaces PhQ and allows less efficient PSI-mediated electron transfer (Lohmann *et al.*, 2006; Fatihi *et al.*, 2015). Addition of vitamin K_1 (PhQ) in the medium allows partial restoration of

the growth of *Chlamydomonas men* mutants in high light, with the exception of *mena* (Figure 4). Although we cannot exclude the possibility that the inability of *Chlamydomonas mena* mutant to recover in the presence of vitamin K_1 is due to a partial deletion in the *HEL22* gene (coding for a DNA helicase RecQ), the fact that the *Synechocystis mena* mutant is also unable to grow on medium supplemented with several naphthoquinone analogs (Johnson *et al.*, 2001) rather suggests that MENA activity might be critical in the assimilation of exogenous PhQ. In this respect, it was demonstrated that *Mycobacterium tuberculosis* treated with a MenA inhibitor could not be rescued completely at high concentrations of exogenous vitamin K_2 (menaquinone-4) (Kurosu and Begari, 2010). We thus hypothesize that the phytyl tail of exogenous PhQ is altered during its assimilation by the cells and that MENA is required to replace the altered phytyl chain. Although this activity has not been yet demonstrated in photosynthetic organisms, the human MenA homolog (UBIAD1) has both side-chain cleavage and prenylation activities (Nakagawa *et al.*, 2010).

In *Chlamydomonas*, the main consequence of loss of PhQ in *menc* (*phyllo*), *mene*, *menb* and *mena* mutants on the organization of the photosynthetic electron transfer chain is a decrease in the amount of functional PSI. This is consistent with the reduced amount of PSI in *Synechocystis* mutants (Johnson *et al.*, 2000, 2003; Sakuragi *et al.*, 2002). Replacement of PhQ by PQ leads to a reduced rate of electron transfer from A_1 to F_X (Lefebvre-Legendre *et al.*, 2007; McConnell *et al.*, 2011). In this respect, the specific increase in PSI antenna size in *men* mutants could represent a compensation mechanism linked to the decrease in the number of active PSI centers. It was previously shown that polypeptides of the PSI LHC (LHCA) accumulate at different levels, and it was suggested that flexibility in LHCA composition would allow adaptation of the PSI antenna configuration to the prevailing environmental conditions (Stauber *et al.*, 2009). The efficiency and maximum electron rate of PSII, however, are diminished proportionally to the PSI decrease in *Chlamydomonas men* mutants, and these effects are exacerbated at higher light intensity where additional effects are observed, such as PSII photoinhibition. Such PSII photoinhibition under high light has been also observed in the Arabidopsis *meng* mutant (Lohmann *et al.*, 2006). In high light, PSI activity in *men* mutants is obviously limited from the acceptor side, a situation that has been described in many studies to lead to PSI photoinhibition and destruction (Munekage *et al.*, 2002; Sommer *et al.*, 2003; Tikkanen *et al.*, 2015). Additionally, the redox state of the PQ pool is more reduced in high light and PQH_2 might occupy the PS1 A_1 site in the *men* mutant, as previously proposed in dark anoxic conditions (McConnell *et al.*, 2011). This might in turn further limit electron transfer and promote photoinhibition.

Critical role of PhQ in photosynthetic electron transfer in anoxia

The four *men* mutants isolated and described in this work were identified by an *in vivo* chlorophyll fluorescence imaging screen based on photosynthetic induction curves following transition from dark anoxia to light (Godaux *et al.*, 2013). This *in vivo* chlorophyll fluorescence screen was originally used to detect mutants impaired in H_2 photoproduction (Godaux *et al.*, 2013), a process that enables algae to initiate their photosynthetic electron transport chain after anoxic incubation when electron acceptors are scarce (Ghysels *et al.*, 2013; Godaux *et al.*, 2013; Clowez *et al.*, 2015). The fluorescence transient observed for hydrogenase-deficient *hydg-2* mutant cells upon the first second of illumination in anoxia (Figure 7a) (Godaux *et al.*, 2013) reflects the reduction phase of PSI acceptors (oxidized ferredoxin and $NADP^+$). Conversely, the lack of change in chlorophyll fluorescence for the *men* mutant in anoxia probably indicates the absence of electron transfer between $P700^+$ and ferredoxin. This is in agreement with the proposal that PQH_2 replaces PhQ in the A_1 site of PSI in anoxia and prevents photosynthetic electron transfer in the *mend* mutant (McConnell *et al.*, 2011). As a result, long-term reactivation (>5 min) of PSII electron transfer in anoxia, which relies on both PSI-dependent hydrogenase activity and PGRL1-dependent PSI cyclic electron flow in wild-type *Chlamydomonas* cells (Godaux *et al.*, 2015), is fully compromised in the *men* mutant (Figure 7b). Loss of PhQ thus severely impairs electron transfer in anoxia in our *men* mutants, as has already been shown in the *mend* mutant (Lefebvre-Legendre *et al.*, 2007; McConnell *et al.*, 2011). Overall these results indicate that the presence of PhQ as a PSI A_1 cofactor is critical in photosynthetic organisms that encounter O_2-deprived conditions on a regular basis.

EXPERIMENTAL PROCEDURES

Strains and growth conditions

The $4A^+$ (*mt*$^+$) and 2′ (*mt*$^-$) wild-type strains used for transformation and genetic crosses, respectively, derive from the 137c reference wild-type strain. The *mend* mutant (Lefebvre-Legendre *et al.*, 2007) was provided by Kevin Redding (Arizona State University, USA). The *C. reinhardtii* strains were grown in TAP medium (Harris *et al.*, 1989) at 25°C under continuous white light (25 μmol photons m^{-2} sec^{-1}), either on solid (1.5% agar) or liquid medium.

Insertional mutagenesis and fluorescence screening procedure

$4A^+$ cells were electroporated with 10 μg of DNA carrier and 250 ng of hygromycin B (*APHVII*) or paromomycin (*APHVIII*) resistance cassettes as previously described (Shimogawara *et al.*, 1998). *APHVII* and *APHVIII* cassettes were amplified by PCR from pHyg3 (Berthold *et al.*, 2002) or pSL18 (Depège *et al.*, 2003)

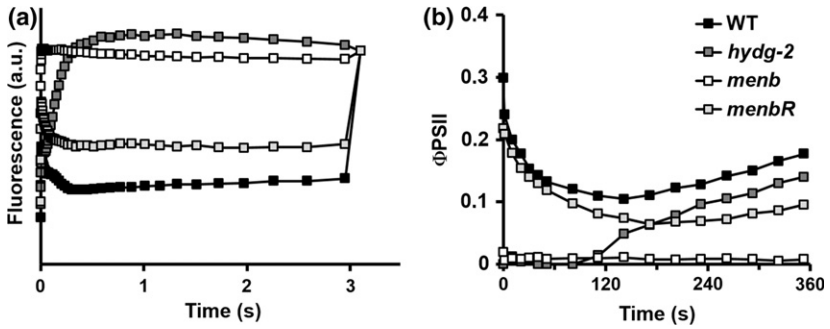

Figure 7. Reactivation of photosynthesis after acclimation to dark anoxia.
(a) Chlorophyll fluorescence induction curves upon illumination at about 110 μmol photons (λ = 520 nm) m^{-2} sec^{-1} of *Chlamydomonas reinhardtii* wild-type (WT), hydrogenase-deficient (*hydg-2*), *menb* mutant and *menbR* complemented strains after acclimation to dark anoxia (220 min).
(b) Evolution of photosystem II quantum yield (ΦPSII) following a shift from dark anoxia to light (250 μmol photons m^{-2} sec^{-1}) of *C. reinhardtii* wild-type, hydrogenase-deficient (*hydg-2*), *menb* mutant and *menbR* complemented strains.

plasmids, respectively, as described in Barbieri *et al.* (2011) using the primers pairs APH7–F/APH7-R for *APHVII* and APH8–F/APH8-R for *APHVIII* (Table S2). Transformants were selected on TAP agar medium containing 25 μg ml^{-1} of hygromycin B or paromomycin in the light. After incubation for 5–10 days under light, transformants were screened directly on transformation plates according to a published procedure (Godaux *et al.*, 2013) in which anoxia is reached by incubation in anoxic bags (Anaerocult P, Merck, http://www.merck.com/).

DNA extraction, PCR amplifications and TAIL-PCR

Total DNA was extracted using the procedure of Newman *et al.* (1990). The PCR amplifications were performed according to standard protocols using Taq polymerase (Promega, http://www.promega.com/) or KAPA HIFI DNA polymerase (KAPA Biosystems, http://www.kapabiosystems.com) for amplification of *MENB* and *MENE* genes using primers menB-F3/menB-R1 and menE-F3/menE-R, respectively (Table S2).

Amplification of the insertion-linked sequence by TAIL-PCR was performed as described previously (Dent *et al.*, 2005) using AD1, AD2 (Liu *et al.*, 1995), RMD227 and RMD228 (Dent *et al.*, 2005) as non-specific primers. For *APHVII*, the specific primers for primary, secondary and tertiary reactions were respectively APH7-R3, APH7-R4 and APH7-R5 at the 5′ end and HygTerm1, HygTerm2 and HygTerm3 at the 3′ end of the coding sequence of the cassette (Table S2). For *APHVIII*, the specific primers for primary, secondary and tertiary reactions were respectively ParoTermB, ParoTermC/1 and ParoTerm2 at the 3′ end of the coding sequence of the cassette (Table S2). The PCR products were sequenced by Beckman Coulter Genomics (http://www.beckmangenomics.com/) and aligned to the *Chlamydomonas* genome sequence database (v.5.5 on PHYTOZOME v11.0).

Genetic analyses

Genetic crosses were performed as described in Duby and Matagne (1999). Zygotes were matured for 3–4 days under continuous light on nitrogen-free minimal agar plates. After maturation, blocks of agar carrying 50–100 zygotes were transferred to fresh TAP agar plates and exposed to chloroform vapor for 30 sec. Germination was induced by exposure to light and restoration of nitrogen. After 10 days of culture, 150–300 meiotic clones were randomly sampled and linkage analysis between resistance cassette and photosynthetic deficiency was determined using the protocol described previously (Godaux *et al.*, 2013).

DNA gel-blot analysis

Total DNA from wild-type and mutants cells was digested with *Stu*I and *Pst*I restriction enzymes (Fast digest, Thermo Scientific, https://www.thermofisher.com/) which do not cut into *APHVII* or *APHVIII* cassettes. DNA was separated on agarose gel, blotted to Hybond-N membranes (Amersham, http://www.gelifesciences.com) and hybridized using digoxigenin-labeled probes (Duby and Matagne, 1999). Probes used to detect *APHVII* and *APHVIII* cassettes were amplified by PCR with the primers HygTail2 and APH7-R2 and pAPH-8F and pAPH-8R (Table S2) using Dig-11 dUTP, according to the procedure recommended by the manufacturer (Roche, http://www.roche.com/).

Spectroscopy

For all experiments, cells grown in low light (25 μmol photons m^{-2} sec^{-1}), were harvested during the exponential growth phase [(3–5) × 10^6 cells ml^{-1}] and concentrated to a concentration of 10 μg chlorophyll ml^{-1} in fresh TAP medium.

In vivo chlorophyll fluorescence measurements were performed at room temperature (25°C) using a fluorescence spectrophotometer (JTS-10, Bio-Logic, http://www.bio-logic.info/) or a fluorescence imaging setup (Speedzen-2, BeamBio, http://www.api-aero.com). Actinic light was provided by light sources peaking at 640 nm and 520 nm, respectively. The effective photochemical yield of PSII (ΦPSII) was calculated as $(F_m' - F_s)/F_m'$, where F_s is the fluorescence level excited by actinic light (I_{lum}), and F_m' is the maximum fluorescence emission level induced by a 150-ms superimposed pulse of saturating light (> 3500 μmol photons m^{-2} sec^{-1}). The relative electron transfer rate is obtained as $rETR_{II} = \Phi PSII \times I_{lum}$ (Genty *et al.*, 1989).

Fluorescence emission spectra at 77 K were recorded using a homebuilt spectrophotometer, based on a detecting diode array (AVS-USB 200; Ocean Optics, http://oceanoptics.com/). The excitation wavelength was provided by a LED source peaking at 440 nm. Cells were treated to induce state transitions before being frozen in liquid nitrogen. The PSII inhibitor DCMU (20 μM) was added for 20 min in the light used to promote state I.

The ratio between active PSI and PSII centers was estimated as previously described (Godaux *et al.*, 2015) on cells adapted to the dark for 30 min. Briefly, the amplitude of the fast phase (<1 ms) of the ECS signal (at 520–546 nm) after illumination with a single-turnover laser flash was monitored with a JTS-10

spectrophotometer (Bio-Logic). The contribution of PSII was calculated from the decrease in the ECS amplitude after the flash upon the addition of the PSII inhibitors DCMU (20 μM) and hydroxylamine (1 mM), whereas the contribution of PSI corresponded to the amplitude of the ECS that was insensitive to these inhibitors. The relative content of PSI was also assessed by measuring P_{700} absorption changes with a probing light peaking at 705 nm (6 nm full width at half maximum). In order to remove unspecific contributions to the signal at 705 nm, absorption changes measured at 740 nm (10 nm full width at half maximum) were subtracted. To fully reduce P_{700}, actinic light was provided by LED light sources (about 1000 μmol photons m^{-2} sec^{-1}) peaking at 640 nm in the presence of DCMU (20 μM) and hydroxylamine (1 mM).

Functional PSI antenna size was measured as the photon absorption rates of PSI (sec^{-1} PS^{-1}) by recording the initial rate of ECS at the onset of actinic light in the presence of the PSII inhibitors DCMU (20 μM) and hydroxylamine (1 mM) (Roberty *et al.*, 2014). The slope was then normalized on ECS values corresponding to one charge separation per PSI.

Western blot analysis

The cell pellet corresponding to 1.5 ml of cell culture was suspended in extraction buffer (SDS 10%, glycerol 10%, 0.1 M DTT, 0.06 M TRIS pH 6.8) to a final concentration of 1 μg protein μl^{-1} and incubated for 5 min at 100°C. Samples (5 μg protein) were then loaded in 10% SDS acrylamide gel and electroblotted according to standard protocols onto PVDF membranes (Amersham GE Healthcare, http://www3.gehealthcare.com/). Detection was performed using a Chemiluminescence Western blotting kit (Roche) with anti-rabbit peroxidase conjugated antibodies. Commercial rabbit antibodies (Agrisera, http://www.agrisera.com/) against PsaA (1:10 000), PsbC (1:30 000) and cytochrome *f* (1:10 000) were used.

Pigment analyses

Pigments were extracted from whole cells in 90% (v/v) methanol, and debris was removed by centrifugation at 10 000 ***g***. The chlorophyll $a + b$ concentration was determined with a λ 20 spectrophotometer (Perkin Elmer, http://www.perkinelmer.com/). Pigments and quinones were extracted from lyophilized cells with *N,N*-dimethylformamide (DMF) (Furuya *et al.*, 1998). The resulting extracts were applied to an Acquity UPLC BEH C18 column (1.7 μm, 2.1 mm × 150 mm, Waters, http://www.waters.com/) at 40°C and were separated at a flow rate of 0.3 ml min^{-1} using an UPLC (Acquity UPLC I-Class system, Waters) coupled with tandem mass spectrometry (Q Exactive, Thermo Scientific). The elution liquid gradient was generated by the following steps using solvent A (formic acid: water = 0.1: 99.9) and solvent B (methanol): 0–5 min, 15% A/85% B to 5% A/95% B, hold to 9 min; 9–10 min, 5% A/95% B to 100% B, hold to 11.5 min; 11.5–12 min, 100% B to 15% A/85% B. The injection volume was 1 μl. Electrospray ionization (ESI) mass spectroscopy measurements were performed in a positive mode.

ACKNOWLEDGEMENTS

We thank K. E. Redding for providing the *mend* strain of *C. reinhardtii*, the laboratory of K. K. Niyogi for providing the $4A^+$ wild-type strain, G. Eppe and A. Marée for their technical help in UPLC-MS analyses, Y. Takahashi for advice on the PhQ extraction method, E. Perez for her help in the identification of putative PTS, F. Franck for assay of PhQ and analysis by HPLC, and M. Radoux for expert technical assistance. PC acknowledges financial support from the Belgian Fonds de la Recherche Scientifique FRS-FNRS (FRFC 2.4597, CDR J.0032, CDR J.0079 and Incentive Grant for Scientific Research F.4520) and from the European Research Council (H2020-EU BEAL project 682580). BE-A is supported by the Belgian FRIA FRS-FNRS. PC is a Research Associate from FRS-FNRS. The authors declare no conflicts of interest.

SUPPORTING INFORMATION

Additional Supporting Information may be found in the online version of this article.

Figure S1. Thermal asymmetric interlaced-PCR product sequences.

Figure S2. Amplification of *MENB* and *MENE* genes and their flanking regions.

Figure S3. Chlorophyll fluorescence induction curves of wild-type and complemented strains.

Figure S4. Relative content of photosystem I.

Figure S5. Determination of photosystem (PS) I and PSII antenna size in wild-type, complemented and *men* mutant strains.

Figure S6. Photosystem (PS) I and PSII content in control and mutant strains.

Figure S7. RT-PCR analysis of *menc* and *mend* mutants.

Figure S8. Sequence alignment of PHYLLO protein from *Chlamydomonas reinhardtii* (CrPHYLLO) and *Arabidopsis thaliana* (AtPHYLLO) with *Escherichia coli* MenF, MenD, MenC and MenH proteins (EcMenF, -D, -C, -H).

Figure S9. Sequence alignment of CYP25 protein from *Chlamydomonas reinhardtii* (CrCYP25) with its two homologs in humans (HsCYP4F2 and CYP4F11).

Table S1. Co-segregation analysis of the antibiotic resistance cassette with the fluorescence phenotype.

Table S2. Primer sequences.

Appendix S1. Detailed description of thermal asymmetric interlaced-PCR analyses.

REFERENCES

Babujee, L., Wurtz, V., Ma, C., Lueder, F., Soni, P., Van Dorsselaer, A. and Reumann, S. (2010) The proteome map of spinach leaf peroxisomes indicates partial compartmentalization of phylloquinone (vitamin K1) biosynthesis in plant peroxisomes. *J. Exp. Bot.* **61**, 1441–1453.

Bailleul, B., Cardol, P., Breyton, C. and Finazzi, G. (2010) Electrochromism: a useful probe to study algal photosynthesis. *Photosynth. Res.* **106**, 179–189.

Barbieri, M.R., Larosa, V., Nouet, C., Subrahmanian, N., Remacle, C. and Hamel, P.P. (2011) A forward genetic screen identifies mutants deficient for mitochondrial complex I assembly in *Chlamydomonas reinhardtii*. *Genetics*, **188**, 349–358.

Berthold, P., Schmitt, R. and Mages, W. (2002) An engineered Streptomyces hygroscopicus aph 7″ gene mediates dominant resistance against hygromycin B in *Chlamydomonas reinhardtii*. *Protist*, **153**, 401–412.

Cardol, P., Gloire, G., Havaux, M., Remacle, C., Matagne, R. and Franck, F. (2003) Photosynthesis and state transitions in mitochondrial mutants of *Chlamydomonas reinhardtii* affected in respiration. *Plant Physiol.* **133**, 2010–2020.

Chen, M., Ma, X., Chen, X., Jiang, M., Song, H. and Guo, Z. (2013) Identification of a hotdog fold thioesterase involved in the biosynthesis of menaquinone in *Escherichia coli*. *J. Bacteriol.* **195**, 2768–2775.

Clowez, S., Godaux, D., Cardol, P., Wollman, F.-A. and Rappaport, F. (2015) The involvement of hydrogen-producing and ATP-dependent NADPH-consuming pathways in setting the redox poise in the chloroplast of *Chlamydomonas reinhardtii* in anoxia. *J. Biol. Chem.* **290**, 8666–8676.

Dent, R.M., Haglund, C.M., Chin, B.L., Kobayashi, M.C. and Niyogi, K.K. (2005) Functional genomics of eukaryotic photosynthesis using insertional mutagenesis of *Chlamydomonas reinhardtii*. *Plant Physiol.* **137**, 545–556.

Depège, N., Bellafiore, S. and Rochaix, J.-D. (2003) Role of chloroplast protein kinase Stt7 in LHCII phosphorylation and state transition in Chlamydomonas. *Science*, **299**, 1572–1575.

Desplats, C., Mus, F., Cuiné, S., Billon, E., Cournac, L. and Peltier, G. (2009) Characterization of Nda2, a plastoquinone-reducing type II NAD(P)H dehydrogenase in chlamydomonas chloroplasts. *J. Biol. Chem.* **284**, 4148–4157.

Drop, B., Webber-Birungi, M., Fusetti, F., Kouřil, R., Redding, K.E., Boekema, E.J. and Croce, R. (2011) Photosystem I of *Chlamydomonas reinhardtii* contains nine light-harvesting complexes (Lhca) located on one side of the core. *J. Biol. Chem.* **286**, 44878–44887.

Duby, F. and Matagne, R.F. (1999) Alteration of dark respiration and reduction of phototrophic growth in a mitochondrial DNA deletion mutant of Chlamydomonas lacking cob, nd4, and the 3′ end of nd5. *Plant Cell*, **11**, 115–125.

Edson, K.Z., Prasad, B., Unadkat, J.D., Suhara, Y., Okano, T., Guengerich, F.P. and Rettie, A.E. (2013) Cytochrome P450-dependent catabolism of vitamin K: ω-hydroxylation catalyzed by human CYP4F2 and CYP4F11. *Biochemistry*, **52**, 8276–8285.

Fatihi, A., Latimer, S., Schmollinger, S., Block, A., Dussault, P.H. and Vermaas, W.F.J. (2015) A dedicated type II NADPH dehydrogenase performs the penultimate step in the biosynthesis of vitamin K1 in Synechocystis and Arabidopsis. *Plant Cell*, **27**, 1730–1741.

Furt, F., Allen, W.J., Widhalm, J.R., Madzelan, P., Rizzo, R.C., Basset, G. and Wilson, M.A. (2013) Functional convergence of structurally distinct thioesterases from cyanobacteria and plants involved in phylloquinone biosynthesis. *Acta. Crystallogr. Sect. D. Biol. Crystallogr.* **69**, 1876–1888.

Furuya, K., Hayashi, M. and Yabushita, Y. (1998) HPLC determination of phytoplankton pigments using N, N-dimethylformamide. *J. Oceanogr.* **54**, 199–203.

Garcion, C., Lohmann, A., Lamodie, E., Catinot, J., Buchala, A., Doermann, P. and Métraux, J.-P. (2008) Characterization and biological function of the ISOCHORISMATE SYNTHASE2 gene of Arabidopsis. *Plant Physiol.* **147**, 1279–1287.

Genty, B., Briantais, J.-M. and Baker, N.R. (1989) The relationship between the quantum yield of photosynthetic electron transport and quenching of chlorophyll fluorescence. *Biochim. Biophys. Acta* **990**, 87–92.

Ghysels, B., Godaux, D., Matagne, R.F., Cardol, P. and Franck, F. (2013) Function of the chloroplast hydrogenase in the microalga Chlamydomonas: the role of hydrogenase and state transitions during photosynthetic activation in anaerobiosis. *PLoS One*, **8**, e64161.

Godaux, D., Emonds-Alt, B., Berne, N., Ghysels, B., Alric, J., Remacle, C. and Cardol, P. (2013) A novel screening method for hydrogenase-deficient mutants in *Chlamydomonas reinhardtii* based on in vivo chlorophyll fluorescence and photosystem II quantum yield. *Int. J. Hydrogen Energy* **38**, 1826–1836.

Godaux, D., Bailleul, B., Berne, N. and Cardol, P. (2015) Induction of photosynthetic carbon fixation in anoxia relies on hydrogenase activity and PGRL1-mediated cyclic electron flow in *Chlamydomonas reinhardtii*. *Plant Physiol.* **168**, 648–658.

Gross, J., Won, K.C., Lezhneva, L., Falk, J., Krupinska, K., Shinozaki, K., Seki, M., Herrmann, R.G. and Meurer, J. (2006) A plant locus essential for phylloquinone (vitamin K1) biosynthesis originated from a fusion of four eubacterial genes. *J. Biol. Chem.* **281**, 17189–17196.

Guergova-Kuras, M., Boudreaux, B., Joliot, A., Joliot, P. and Redding, K. (2001) Evidence for two active branches for electron transfer in photosystem I. *Proc. Natl Acad. Sci. USA* **98**, 4437–4442.

Harris, E.H., Burkhart, B.D., Gillham, N.W. and Boynton, J.E. (1989) Antibiotic resistance mutations in the chloroplast 16S and 23S rRNA genes of *Chlamydomonas reinhardtii*: correlation of genetic and physical maps of the chloroplast genome. *Genetics*, **123**, 281–292.

Hippler, M., Redding, K. and Rochaix, J.D. (1998) Chlamydomonas genetics, a tool for the study of bioenergetic pathways. *Biochim. Biophys. Acta* **1367**, 1–62.

Ikeda, Y., Komura, M., Watanabe, M., Minami, C., Koike, H., Itoh, S., Kashino, Y. and Satoh, K. (2008) Photosystem I complexes associated with fucoxanthin-chlorophyll-binding proteins from a marine centric diatom, *Chaetoceros gracilis*. *Biochim. Biophys. Acta – Bioenerg.* **1777**, 351–361.

Jiang, M., Cao, Y., Guo, Z., Chen, M., Chen, X. and Guo, Z. (2007) Menaquinone biosynthesis in *Escherichia coli*: identification of 2-Succinyl-5-enolpyruvyl-6-hydroxy-3-cyclohexene-1-carboxylate as a novel intermediate and re-evaluation of MenD activity†. *Biochemistry*, **46**, 10979–10989.

Jiang, M., Chen, X., Guo, Z., Cao, Y., Chen, M. and Guo, Z. (2008) Identification and characterization of (1R, 6R) -2-Succinyl-6-hydroxy-2,4-cyclohexadiene-1-carboxylate synthase in the menaquinone biosynthesis of *Escherichia coli*. *Biochemistry*, **47**, 3426–3434.

Johnson, T.W., Shen, G., Zybailov, B. *et al.* (2000) Recruitment of a foreign quinone into the A1 site of photosystem I. I. genetic and physiological characterization of phylloquinone biosynthetic pathway mutants in Synechocystis sp. PCC 6803. *J. Biol. Chem.* **275**, 8523–8530.

Johnson, T.W., Zybailov, B., Jones, A.D., Bittl, R., Zech, S., Stehlik, D., Golbeck, J.H. and Chitnis, P.R. (2001) Recruitment of a foreign quinone into the A1 site of photosystem I: in vivo replacement of plastoquinone-9 by media-supplemented naphthoquinones in phylloquinone biosynthetic pathway mutants of synechocystis sp. PCC 6803. *J. Biol. Chem.* **276**, 39512–39521.

Johnson, T.W., Naithani, S., Stewart, C., Zybailov, B., Jones, A.D., Golbeck, J.H. and Chitnis, P.R. (2003) The menD and menE homologs code for 2-succinyl-6-hydroxyl-2,4-cyclohexadiene-1-carboxylate synthase and O-succinylbenzoic acid-CoA synthase in the phylloquinone biosynthetic pathway of Synechocystis sp. PCC 6803. *Biochim. Biophys. Acta – Bioenerg.* **1557**, 67–76.

Joliot, P. and Joliot, A. (1999) In vivo analysis of the electron transfer within photosystem I: are the two phylloquinones involved? *Biochemistry*, **38**, 11130–11136.

Kim, H.U. (2008) The AAE14 gene encodes the Arabidopsis o-succinylbenzoyl- CoA ligase that is essential for phylloquinone synthesis and photosystem-I function. *Plant J.* **54**, 272–283.

Kurosu, M. and Begari, E. (2010) Vitamin K2 in electron transport system: are enzymes involved in vitamin K2 biosynthesis promising drug targets? *Molecules*, **15**, 1531–1553.

Lauersen, K.J., Willamme, R., Coosemans, N., Joris, M., Kruse, O. and Remacle, C. (2016) Peroxisomal microbodies are at the crossroads of acetate assimilation in the green microalga *Chlamydomonas reinhardtii*. *Algal Res.* **16**, 266–274.

Law, A., Thomas, G. and Threlfall, D.R. (1973) 5′-Monohydroxyphylloquinone from Anacystis and Euglena. *Phytochemistry*, **12**, 1999–2004.

Lefebvre-Legendre, L., Rappaport, F., Finazzi, G., Ceol, M., Grivet, C., Hopfgartner, G. and Rochaix, J.D. (2007) Loss of phylloquinone in Chlamydomonas affects plastoquinone pool size and photosystem II synthesis. *J. Biol. Chem.* **282**, 13250–13263.

Liu, Y.G., Mitsukawa, N., Oosumi, T. and Whittier, R.F. (1995) Efficient isolation and mapping of *Arabidopsis thaliana* T-DNA insert junctions by thermal asymmetric interlaced PCR. *Plant J.* **8**, 457–463.

Lohmann, A., Schöttler, M.A., Bréhélin, C., Kessler, F., Bock, R., Cahoon, E.B. and Dörmann, P. (2006) Deficiency in phylloquinone (vitamin K1) methylation affects prenyl quinone distribution, photosystem I abundance, and anthocyanin accumulation in the Arabidopsis AtmenG mutant. *J. Biol. Chem.* **281**, 40461–40472.

McConnell, M.D., Cowgill, J.B., Baker, P.L., Rappaport, F. and Redding, K.E. (2011) Double reduction of plastoquinone to plastoquinol in Photosystem 1. *Biochemistry*, **50**, 11034–11046.

Meganathan, R. (2001) Biosynthesis of menaquinone (vitamin K2) and ubiquinone (coenzyme Q): a perspective on enzymatic mechanisms. *Vitam. Horm.* **61**, 173–218.

Munekage, Y., Hojo, M., Meurer, J., Endo, T., Tasaka, M. and Shikanai, T. (2002) PGR5 is involved in cyclic electron flow around photosystem I and is essential for photoprotection in Arabidopsis. *Cell*, **110**, 361–371.

Nakagawa, K., Hirota, Y., Sawada, N., Yuge, N., Watanabe, M., Uchino, Y., Okuda, N., Shimomura, Y., Suhara, Y. and Okano, T. (2010) Identification of UBIAD1 as a novel human menaquinone-4 biosynthetic enzyme. *Nature*, **468**, 117–121.

Newman, S.M., Boynton, J.E., Gillham, N.W., Randolph-Anderson, B.L., Johnson, A.M. and Harris, E.H. (1990) Transformation of chloroplast ribosomal RNA genes in Chlamydomonas: molecular and genetic characterization of integration events. *Genetics*, **126**, 875–888.

Omata, T. and Murata, N. (1984) Cytochromes and prenylquinones in preparations of cytoplasmic and thylakoid membranes from the

cyanobacterium (blue-green alga) *Anacystis nidulans*. *Biochim. Biophys. Acta* **766**, 395–402.

Ozawa, S.I., Kosugi, M., Kashino, Y., Sugimura, T. and Takahashi, Y. (2012) 5′-monohydroxyphylloquinone is the dominant naphthoquinone of PSI in the green alga *Chlamydomonas reinhardtii*. *Plant Cell Physiol.* **53**, 237–243.

Reumann, S., Babujee, L., Ma, C., Wienkoop, S., Siemsen, T., Antonicelli, G.E., Rasche, N., Lüder, F., Weckwerth, W. and Jahn, O. (2007) Proteome analysis of Arabidopsis leaf peroxisomes reveals novel targeting peptides, metabolic pathways, and defense mechanisms. *Plant Cell*, **19**, 3170–3193.

Roberty, S., Bailleul, B., Berne, N., Franck, F. and Cardol, P. (2014) PSI Mehler reaction is the main alternative photosynthetic electron pathway in Symbiodinium sp., symbiotic dinoflagellates of cnidarians. *New Phytol.* **204**, 81–91.

Rochaix, J.-D. (2002) Chlamydomonas, a model system for studying the assembly and dynamics of photosynthetic complexes. *FEBS Lett.* **529**, 34–38.

Sakuragi, Y., Zybailov, B., Shen, G. *et al.* (2002) Insertional inactivation of the menG Gene, encoding 2-Phytyl-1, 4-naphthoquinone methyltransferase of Synechocystis sp. PCC 6803, results in the incorporation of 2-phytyl-1, 4-naphthoquinone into the A 1 site and alteration of the equilibrium constant between A1 and FX in photosystem I. *Biochemistry* **41**, 394–405.

Semenov, A.Y., Vassiliev, I.R., Van Der Est, A., Mamedov, M.D., Zybailov, B., Shen, G., Stehlik, D., Diner, B.A., Chitnis, P.R. and Golbeck, J.H. (2000) Recruitment of a foreign qiunone into the a(1) site of photosystem I: Altered kinetics of electron transfer in phylloquinone biosynthetic pathway mutants studied by time-resolved optical, EPR, and electrometric techniques. *J. Biol. Chem.* **275**, 23429–23438.

Shimada, H., Ohno, R., Shibata, M., Ikegami, I., Onai, K., Ohto, M.A. and Takamiya, K.I. (2005) Inactivation and deficiency of core proteins of photosystems I and II caused by genetical phylloquinone and plastoquinone deficiency but retained lamellar structure in a T-DNA mutant of Arabidopsis. *Plant J.* **41**, 627–637.

Shimogawara, K., Fujiwara, S., Grossman, A. and Usuda, H. (1998) High-efficiency transformation of *Chlamydomonas reinhardtii* by electroporation. *Genetics*, **148**, 1821–1828.

Sommer, F., Hippler, M., Biehler, K., Fischer, N. and Rochaix, J.-D. (2003) Comparative analysis of photosensitivity in photosystem I donor and acceptor side mutants of *Chlamydomonas reinhardtii*. *Plant, Cell Environ.* **26**, 1881–1892.

Stauber, E.J., Busch, A., Naumann, B., Svatos, A. and Hippler, M. (2009) Proteotypic profiling of LHCI from *Chlamydomonas reinhardtii* provides new insights into structure and function of the complex. *Proteomics*, **9**, 398–408.

Takahashi, H., Clowez, S., Wollman, F.-A., Vallon, O. and Rappaport, F. (2013) Cyclic electron flow is redox-controlled but independent of state transition. *Nat. Commun.* **4**, 1954. doi:10.1038/ncomms2954.

Tikkanen, M., Rantala, S. and Aro, E.-M. (2015) Electron flow from PSII to PSI under high light is controlled by PGR5 but not by PSBS. *Front. Plant. Sci.* **6**, 521. doi:10.3389/fpls.2015.00521.

Widhalm, J.R., van Oostende, C., Furt, F. and Basset, G.J.C. (2009) A dedicated thioesterase of the Hotdog-fold family is required for the biosynthesis of the naphthoquinone ring of vitamin K1. *Proc. Natl Acad. Sci. USA* **106**, 5599–5603.

Widhalm, J.R., Ducluzeau, A.L., Buller, N.E., Elowsky, C.G., Olsen, L.J. and Basset, G.J.C. (2012) Phylloquinone (vitamin K1) biosynthesis in plants: two peroxisomal thioesterases of lactobacillales origin hydrolyze 1,4-dihydroxy-2-naphthoyl-coa. *Plant J.* **71**, 205–215.

Wollman, F.A. (2001) State transitions reveal the dynamics and flexibility of the photosynthetic apparatus. *EMBO J.* **20**, 3623–3630.

Yoshida, E., Nakamura, A. and Watanabe, T. (2003) Reversed-phase HPLC determination of chlorophyll a′ and naphthoquinones in photosystem I of red algae: existence of two menaquinone-4 molecules in photosystem I of Cyanidium caldarium. *Anal. Sci.* **19**, 1001–1005.

Ziegler, K., Maldener, I. and Lockau, W. (1989) 5′-monohydroxyphylloquinone as a component of photosystem I. *Zeitschrift fur Naturforsch – Sect. C. J. Biosci.* **44**, 468–472.